



25<sup>th</sup> ABCM International Congress of Mechanical Engineering  
October 20-25, 2019, Uberlândia, MG, Brazil

## COB-2019-1202

# ADHESIVE JOINTS CHARACTERIZATION USING THE MMB-MIXED MODEL BENDING TEST

**Felipe Pereira da Silva**

**Eduardo Martins Sampaio**

Universidade do Estado do Rio de Janeiro, Instituto Politécnico – Nova Friburgo, RJ, Brasil

fps.felipesilva@gmail.com

edu.msampaio@gmail.com

**Ranulfo Martins Carneiro Neto**

Universidade Federal do Rio de Janeiro – Macaé, RJ, Brasil

ranulfocarneiro@yahoo.com.br

**Abstract.** *The use of structural adhesives has increased in many fields of modern engineering, one of the main reasons for this growth is related to their properties when compared to other conventional joining methods. In this work we study the behavior of mixed load adhesive joints (Mode I and Mode II) by reproducing the Mixed Modeling test, registered in ASTM D6671 / D6671M (Mixed Mode I-Mode II Interlaminar Fracture Toughness of Unidirectional Fiber Reinforced Polymer Matrix Composites). For the study, 1.6mm thick metal-metal specimens were considered and the 0.9mm thick ARC 858 adhesive was used as adhering agent. The Conformed Based Beam Method (CBBM) was applied to the experiment to get fracture toughness. It presents a mathematical model independent of the crack propagation follow-up, and the experiment depends only on the P load, monitored by the universal testing machine and the deformations in mode I ( $\delta I$ ) and mode II ( $\delta II$ ), which are monitored by two dials gauges. Thus, it is allowed to evaluate the efficiency of the method employed and make a new test concept available to the Adhesion and Adherence Laboratory (AAL).*

**Keywords:** *MMB – mixed model mending, bonded joints, adhesion and adherence*

## 1. INTRODUCTION

Sampaio (1998) said that bonded joints, which are the joints of materials through adhesives, are designed for high shear strength. The use and study of these adhesive joints has been increasing in recent years due to their peculiar characteristics when compared to conventional methods of joining materials such as screw, rivets and welds.

Nunes (2017) explained that under actual application conditions, many of these adhesive joints will be subject to mixed loading stresses (Mode I and Mode II). There are several tests developed for testing mixed mode adhesive joints. They are tests similar to pure mode I and II, differing in the way the load is applied or in the symmetry / asymmetry of the specimens, in order to combine both modes.

Nunes (2017) stated that some of these tests allow you to vary the ratio between mode I and II and thus study the influence of this ratio on joint strength. From the results obtained, it is usually observed that the fracture resistance increases with the percentage of mode II.

As there are still few of these methods for characterization of mixed loading adhesive joints available in the literature, this paper aims to present the survey of specific properties of adhesive joints, using the mixed loading test MMB - Mixed Model Bending. Which is represented by ASTM D6671 / D6671M and is the only standardized test for this type of survey.

Conventionally, the DCB-Double Cantiliver Beam and ENF-End-Notched Flexure tests have been widely used to survey fracture toughness under mode I and mode II. The present work aims to use the MMB-Mixed Model Bending apparatus to gather in a single method the possibility of study these properties of adhesive joints, thus optimizing the characterization process and cost in the production of specimens.

## 2. EXPERIMENTAL

### 2.1 MMB – Mixed Model Bending

For the experiment, the MMB - Mixed Model Bedding apparatus was designed and reproduced according to dimensions and specifications of ASTM D6671 / D6671M, which is represented by Fig. 1 (a).

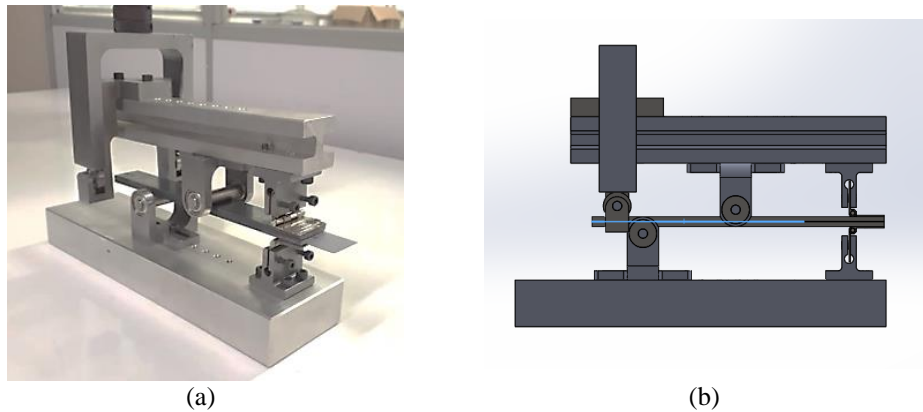


Figure 1. MMB apparatus, (a) isometric view e (b) side view

This test is about adding a load that causes an opening mode to a mid-span ENF specimen, as shown in Fig. 2 (b). This additional load causes the arms to separate as as in the DCB test. According with Crews and Reeder (1988), the relative value of the two applied forces determines the degree of mixed mode at the crack end. Both the force applied to the specimen through the apparatus arm and the bending force will be generated from a single load application  $P$ , as shown in Fig. 2 (b).

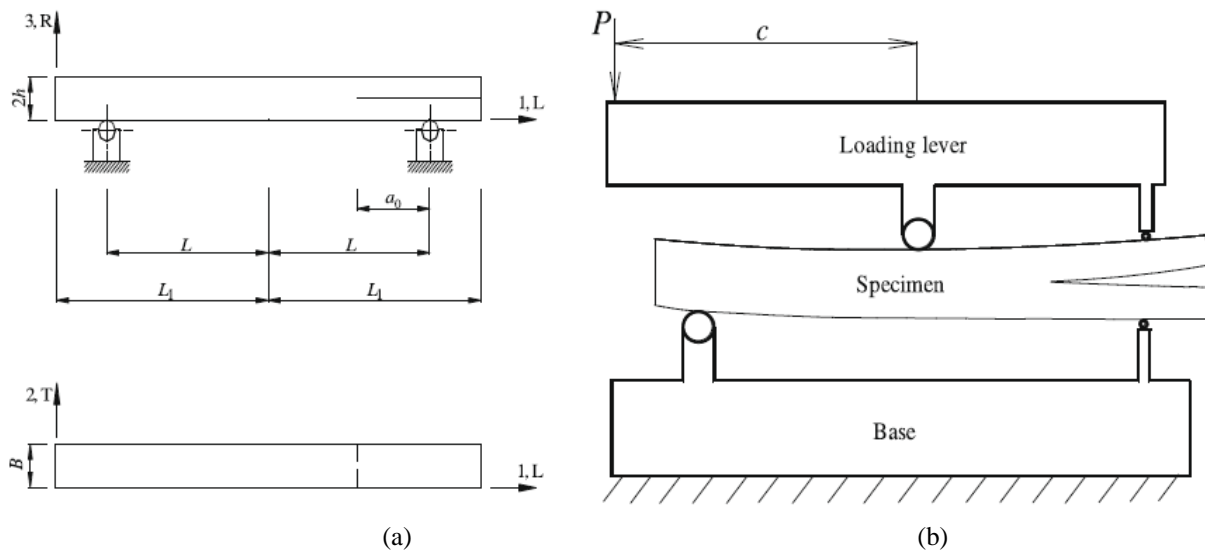


Figure 2. MMB operation

Available in: <https://www.sciencedirect.com/science/article/pii/S0013794409002902>

The apparatus presents a number of possibilities of point of application of the load  $P$  through the arm, the results being obtained depending on the configuration of the distance  $c$  in relation to the point of application  $P$ , thus varying the resulting moment in the specimen.

## 2.2 Materials

The specimen to be tested, shown in Fig. 3, is made of 2 identical steel bars with the following dimensions: width (b) 25.4 mm, length ( $2 \times L_1$ ) 200 mm and thickness 1.6 mm. The specimen bonded with a 0.9mm thick adhesive will have a total average thickness ( $2h$ ) of 4.1mm.

Initially, the carbon steel hinges were separated and sanded with an MBX pneumatic sander for bonding to the external surface of the specimen. These hinges will be one of the main contact points for applying stress to the specimen, due to which the industrial AralditeHobby® was used as adhesive in the fixing of these hinges, Fig. 3.



Figure 3. Specimen

Prior to bonding the hinges, the specimens were blasted with G40 steel grit on the inner surfaces to provide a surface roughness, then the parts were cleaned with acetone to receive the ARC 858 adhesive.

The ARC 858 adhesive provided by Chesterton is an adhesive used to protect metal surfaces from corrosion, erosion or chemical attack, and also helps to rebuild surfaces with a strong protection that in some cases surpass weld restoration. The ARC 858 properties provided by the manufacturer are presented in Table 1 below.

Table 1. Properties of ARC 858 supplied by the manufacturer.

Property	Base Standard For Determination	Values
Compressive Strength	ASTM D 695	89.24 MPa
Bending Strength	ASTM D 790	60.80 MPa
Bending Modulus	ASTM D 790	6766.59 MPa
Tensile Strength	ASTM D 638	42.17 MPa
Hockwell Hardness	ASTM D 785	R105

Available in: [http://www.btdt.uerj.br/tde\\_busca/processaPesquisa.php?pesqExecutada=1&id=7460&PHPSESSID=epihr53ghcn0i17huod2is85c3](http://www.btdt.uerj.br/tde_busca/processaPesquisa.php?pesqExecutada=1&id=7460&PHPSESSID=epihr53ghcn0i17huod2is85c3)

For adhesive bonding, two steel jamb have been developed to provide a thickness on the adhesive ( $t$ ) of 0.9 mm, as well as the introduction of the 55 mm pre-crack ( $a$ ) and the initial pre-crack ( $a_0$ ) with 30mm counted from the hinge to the adhesive region. The first template was positioned at the opposite end with respect to the hinges and has the following dimensions: 10x25x0.9 mm, although this jamb generates a pre-crack at the tip of the specimen, the crack will have no impeding or modifying properties the test results. The second jamb was responsible for creating the pre-crack, with the dimensions: ( $a_0$ ) 80mmx25x0,9 mm. Both specimen jams and characteristics are shown in Fig. 4.

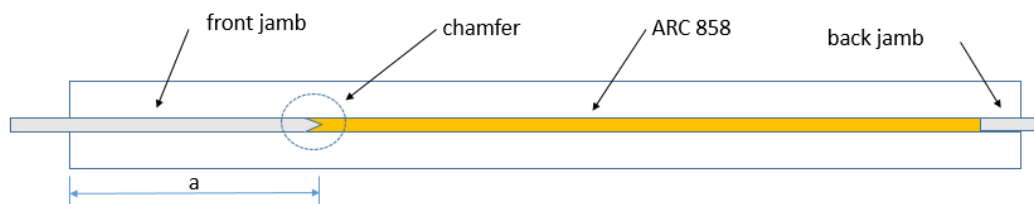


Figure 4. Specimen

On the front jambs the crack length was marked  $a = 55\text{mm}$  and a chamfer were machined the tip next to the adhesive on both sides of the workpiece. This chamfer (see Fig. 4) was employed to further reduce the possibility of initiating a fracture at the adhesive-bond interface, inducing the crack to propagate cohesively throughout the test.

After bonding the substrates and hinges, the 5 specimens were measured to record and survey the information required for the MMB assay. These measures are presented through Tab.2.

Table 2. Specimen information and measurements after the curing process

Specimen	Width (mm)	Length (mm)	Thickness (mm)	Pre-crack (mm)	Adhesive thickness (mm)	a0 (mm)	h (mm)
1	25.0	200.1	4.1	56.6	0.9	29.1	2.03
2	25.0	200.2	4.1	54.2	0.9	29.9	2.05
3	24.7	199.9	4.0	53.0	0.8	30.7	1.98
4	24.8	199.8	3.9	53.2	0.7	29.5	1.95
5	24.7	200.0	4.1	53.2	0.9	29.5	2.07
Average (mm)	24.8	200.0	4.1	53.2	0.9	29.5	2.00
Standard Deviation	0.2 (0.8%)	0.2 (0.1%)	0.1 (2.4%)	1.5 (2.8%)	0.1 (11.1%)	0.6 (2.0%)	0.05 (2.5%)

### 2.3 Methodology

Moura et al (2007) also realized that as with the methods for the DCB and ENF tests, the beam theory does not take into account the FPZ-Fracture Process Zone or the crack region. Thus, he developed the study to determine  $G_{Ic}$  and  $G_{IIc}$  applying the concepts of equivalent crack length in the MMB test. This method is called the CBBM - Compliance-Based Beam Method.

The determination of the energy release rate is based on the beam theory. Figure 5 shows the loading mode of the MMB test as a function of applied load,  $P$ , length of load arm  $c$ , and half the length of specimen,  $L$ .

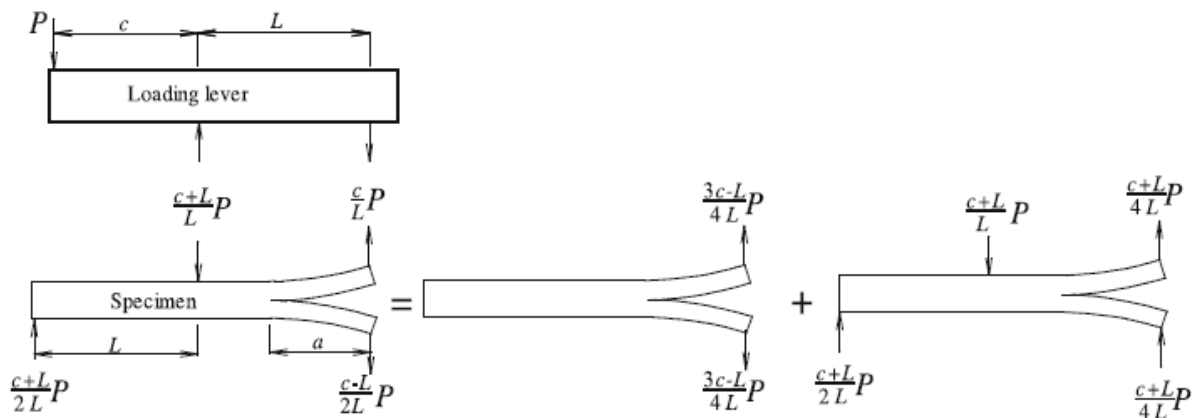


Figure 5. Specimen efforts for the MMB test

Available in: <https://www.sciencedirect.com/science/article/pii/S0013794409002902>

As shown in Fig. 5, the component for mode I and II is represented by Eq. (1) and (2), respectively.

$$P_{II} = \left( \frac{c-L}{L} \right) P \quad (1)$$

$$P_{II} = \left( \frac{c-L}{L} \right) P \quad (2)$$

For an initial understanding, Moura combines the pure modes of the DCB and ENF tests presented in Fig. 5 and applying *Castigliano's Theorem*, we get the Eq. (3) and (4) for the flexibilities ( $C_I$  and  $C_{II}$ ) of the test.

$$C_I = \frac{\delta_I}{P_I} = \frac{8a^3}{E_1 B h^3} + \frac{12a}{5G_{13} B h} \quad (3)$$

$$C_{II} = \frac{\delta_{II}}{P_{II}} = \frac{3a^3 + 2L^3}{8E_1 B h^3} + \frac{3L}{10G_{13} B h} \quad (4)$$

The deformation  $\delta_{II}$  is obtained by  $\delta_{II} = \delta_c + \delta I/4$ , where  $\delta_c$  is the displacement measured in the middle of the specimen at the point of load application and  $\delta I$  is the displacement measured at the beginning of the specimen, in the region of application of the specimen load in mode I.

There are several aspects not included in Eq. (2) and Eq. (4) that may influence the behavior of the specimen. Indeed, issues such as stress concentrations, the presence of the adhesive layer and the existence of the FPZ zone in front of the crack tip during propagation are not included in these equations, which influences the absorption of part of the test energy. To overcome this limitation, De Moura et al. (2008) proposes the use of  $E_{fI}$  and  $E_{fII}$  (Eq. (5) and Eq. (7)) to be substituted in the equations of  $C_I$  and  $C_{II}$  respectively in place of the elasticity modules in the longitudinal direction  $E_I$ .

$$E_{fI} = \left( C_{0I} - \frac{12(\alpha_0 + h|\Delta_I|)}{5BhG_{13}} \right)^{-1} \frac{8(\alpha_0 + h|\Delta_I|)^3}{Bh^3} \quad (5)$$

where

$$\Delta_I = h \sqrt{\frac{E}{11G_{13}} \left[ 3 - 2 \left( \frac{\Gamma}{1 + \Gamma} \right)^2 \right]}, \quad \Gamma = 1.18 \frac{E}{G_{13}} \quad (6)$$

$$E_{fII} = \frac{3\alpha_0^3 + 2L^3}{8Bh^3} \left( C_{0II} - \frac{3L}{10BhG_{13}} \right)^{-1} \quad (7)$$

The equivalent mode I crack length can be obtained from the Eq. (8), Eq. (9) and Eq. (10).

$$\alpha_{eql} = \alpha + h|\Delta| + \Delta\alpha_{FPZ} = \frac{1}{6\alpha} A' - \frac{2\beta}{A'} \quad (8)$$

where

$$\alpha = \frac{8}{Bh^3 E_{fI}}; \quad \beta = \frac{12}{5BhG_{13}}; \quad \gamma = -C_I \quad (9)$$

$$A' = \left( \left( -108 \gamma + 12 \sqrt{3 \left( \frac{4\beta^3 + 27\gamma^2\alpha}{\alpha} \right)} \right) \alpha^2 \right)^{\frac{1}{3}} \quad (10)$$

The equivalent mode II crack length can be obtained from the Eq. (11) and Eq.(12).

$$\alpha_{eqlII} = \alpha + \Delta_{FPZ} = \left[ \frac{C_{IIcorr}}{C_{0IIcorr}} \alpha_0^3 + \frac{2}{3} \left( \frac{C_{IIcorr}}{C_{0IIcorr}} - 1 \right) L^3 \right]^{\frac{1}{3}} \quad (11)$$

where

$$C_{IIcorr} = C_{II} - \frac{3L}{5G_{13} Bh} \quad e \quad C_{0IIcorr} = C_{0II} - \frac{3L}{5G_{13} Bh} \quad (12)$$

Thus, De Moura et al.(2010) arrives in Eq. (13) and Eq. (14) for calculating fracture toughness in mode I and mode II,  $G_{Ic}$  and  $G_{IIc}$  respectively, which do not need crack monitoring during the test. Being the experiment dependent only on the applied P load, collected from the Universal Test Machine and the deformations  $\delta I$  and  $\delta_{II}$ . The first being measured at the distance of the vertical crack opening measured parallel to the hinge region, the second being measured at the center of the specimen, corresponding to flexion from the application of the central pin load of the MMB experiment.

$$G_I = \frac{12\alpha_{eql}^2 P_I^2}{B^2 h^3 E_{fI}} \quad (13)$$

$$G_{II} = \frac{9\alpha_{eqlII}^2 P_{II}^2}{16B^2 h^3 E_{fII}} \quad (14)$$

In addition to the calculations presented, it is important to know the degree of mix or ratio  $\phi$  of the test (Eq.15), which is the main factor in the classification of the predominant amount of effort present in mode I or mode II.

$$\phi = \tan^{-1} \left[ \frac{K_{II}}{K_I} \right] = \tan^{-1} \sqrt{\left( \frac{G_{II}}{G_I} \right)} \quad (15)$$

The ratio degree is directly proportional to the fracture toughness in mode II and inversely proportional to mode I. Its maximum value is 90.

## 2.4 Experiment

To perform the test, a SHIMADZU® Universal Test Machine (Fig.6) with a 5kN load cell, made available by the TECPOL IPRJ laboratory, was used.



Figure 6. Experiment representation

In order to solve the problem of crack propagation measurement and consequently the measurements of  $\delta I$  and  $\delta II$  displacements, a new methodology was developed with the mechanisms available in the AAL, through dials gauges and recording of displacements through Samsung® cell phone camera shooting, model J5Prime. Using the software that is interconnected with the test machine, it was possible to record the real-time test run and the creation of the P- $\delta$  curve. To perform the test near the static conditions, the crossbar displacement rate according to ASTM D6671 / D6671M Standard must be 0.5mm/min, which was used in this work.

Before starting the test, measurements were made for the load application distance (c) and the value of the load application distance PII to the hinge, called distance L. Being c equal to 93.5 mm and L equal to 64.0 mm, values which are associated for the use of the CBBM method.

The recording of the data obtained from the footage was applied in an Excel spreadsheet and treated with the CBBM methodology equations. At first, the first dial gauge (the left of figure 6) was used as a reference, being recorded the deformations in the dial gauge and the load P (load figure at the bottom of figure 6) as the first dial gauge advanced every 0,1 mm. It is important to note that the deformation record was only started after the upper fork was accommodated in the MMB apparatus bearings, considering at this moment of accommodation the zero points in the two comparator clocks, taking these as the reference base in the measurements.

All tests were performed at room temperature of 21.3 ° C, with 55% relative humidity.

## 3. RESULTS AND DISCUSSION

Using the CBBM method it was allowed to calculate the PI and PII load, and the deformation  $\delta I$  and  $\delta II$  were monitored every 0.1 mm recorded in the dial gauge near the hinge of Fig. 6. From these values, the curve is constructed. P- $\delta$  or R curve for a ratio of 24.7°, Fig. 7. The values of loads (PI and PII) and deformations ( $\delta I$  and  $\delta II$ ) were entered in an Excel spreadsheet and associated the equations for the CBBM method with the values of Tab. 2 of the present work. Thus, it was possible to locate the fracture toughness values in mode I and II in the MMB test as shown in Fig.8 and Fig. 9.

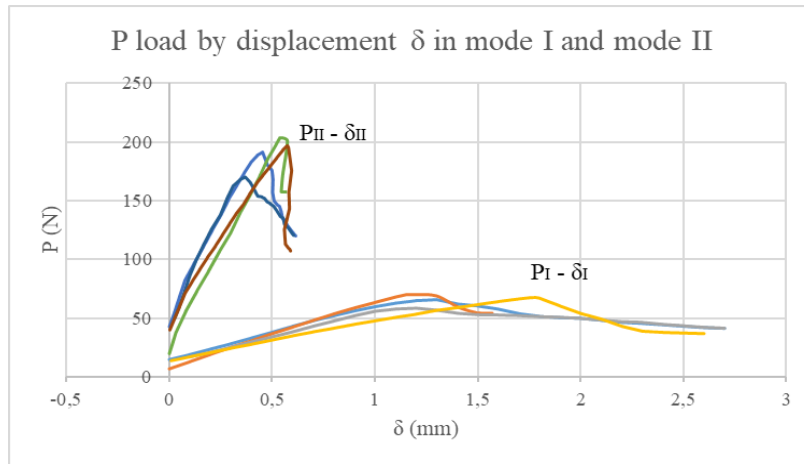


Figure 7. R curve - PI and PII load by  $\delta I$  and  $\delta II$  deformation

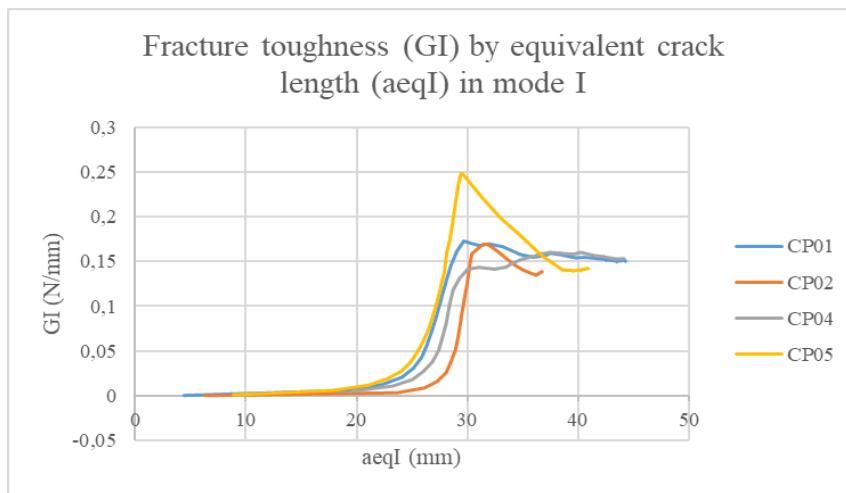


Figure 8. Fracture toughness graph under equivalent crack length in mode I

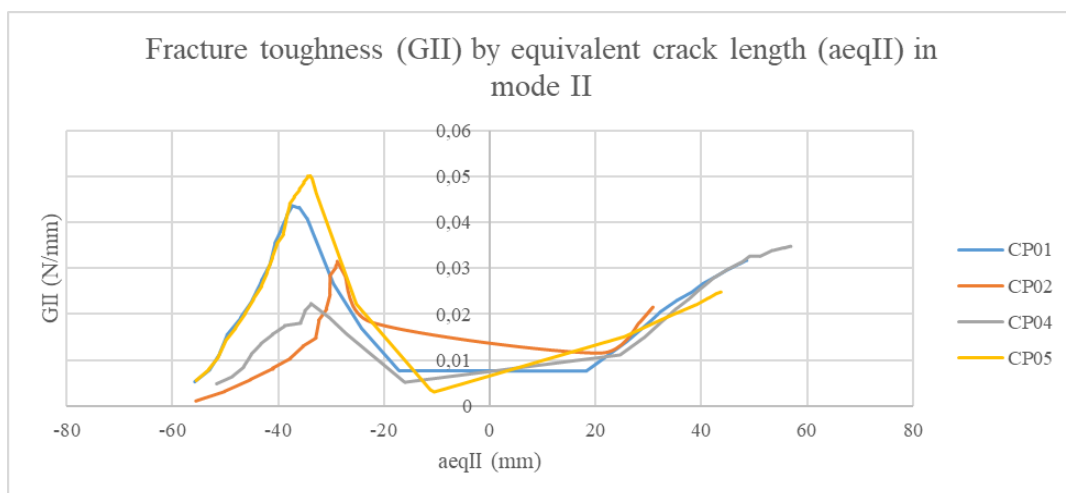


Figure 9. Fracture toughness graph under mode II equivalent crack length

R-curves for all specimens were obtained considering the CBBM described. The peaks of these R-curves actually allow the representation of the deformation energy components as a function of their equivalent slot length, thus allowing an easy identification of each deformation energy component (Fig. 7) and its mode ratio during fracture growth.

The fracture toughness values obtained for the four test specimens are shown in Tab. 3.

Table 3 – Fracture toughness results in mode I and II

Specimen	G <sub>Ic</sub> (N/mm)	G <sub>IIc</sub> (N/mm)
CP01	0.1729	0.0437
CP02	0.1688	0.0315
CP04	0.1605	0.0348
CP05	0.2482	0.0502
Average	0.1876	0.0401
Standard Deviation	0.0407	0.0085

Table 4 – Comparison between MMB, ATDCB, DCB and ENF results for different authors.

Test	Degree of ratio $\phi$	Autor	Adhesive	G <sub>Ic</sub> (N/mm)	G <sub>IIc</sub> (N/mm)	Adhesive thickness (mm)
ATDCB	23,6	Nunes, 2017	Araldite AV138	0,099	0,019	1
ATDCB	23,9	Nunes, 2017	Araldite 2015	0,422	0,083	1
ATDCB	25,0	Esteves,2010	Araldite 2015	0,320	0,070	0,2
DCB e ENF	Modo Puro	Neto,2017	ARC 858	0,135	2,025	0,4
DCB e ENF	Modo Puro	Esteves,2010	Araldite 2015	0,440	2,100	0,2
MMB	24,7	Silva, 2019	ARC 858	0,188	0,040	0,9

With the authors selected above, it was possible to identify the experiments with the pure loading test or with mode II fracture toughness values are diferents when compared to the G<sub>IIc</sub> values of the mixed loading test. This divergence is available with a load application in mode II.

Since these adhesive joints are much more resistant to shear stress than tensile strength, it is understood that for ENF tests the application of the load occurs at the center of the specimen, resulting that all the effort / energy to break the shear bond was employed in a single mode. The mentioned mixed load tests performed predominantly in mode I, which requires lower energy to perform joint damage.

#### 4. CONCLUSION

The present work was carried out to characterize the fracture behavior of adhesive joints of metallic substrates. The obtained data allowed to study the fracture behavior of a commercial epoxy adhesive, when submitted to mixed loading requests (I + II). For this, a project was developed in Solidworks2014 software to reproduce the MMB apparatus according to ASTM D6671 / D6671M.

Results for the MMB test when compared with other authors, were found to be satisfactory for mode I loading, with an average of G<sub>Ic</sub> of 0.188 N/mm for the four specimens tested. However, when comparing the values of G<sub>IIc</sub>, an average of 0.04 N/mm, the values differed greatly for the values of the ENF test, having a 98% reduction in the comparison of averages.

Due to this, other authors were sought to compare the results of mixed loading tests with the DCB and ENF tests. Thus, when comparing the values of a pure mode II ENF test with those of the mixed mode test (MMB and ATDCB), with a ratio between 24 and 25°, these values were much higher than the G<sub>Ic</sub> values for mixed loading tests. When comparing the DCB test with the mixed loading test the values show satisfactory results for mode I fracture toughness (G<sub>Ic</sub>). Thus revealing that the degree of ratio factor  $\phi$  is very important for comparing the experimental results, it is necessary to construct a GI-GII curve for the real knowledge of the energies applied to a given adhesive, resulting in the values of the curve values. DCB and ENF for pure modes I and II, respectively. Due to this, it was concluded that in an adhesive joint project it is very important to have as premise the type of effort to be employed or predominant in the project, which will determine its degree of ratio/mix. Thus identifying that this area of study is on the rise and there is a great need for the development of new technologies for mix type identification in an adhesive joint project, as the majority of adhesive joints will work under mixed loading.

In addition, when performing the mode II fracture toughness curve (GII) by the CBBM method, which considers the equivalent mode II crack length (aeq II), a negative region was identified in the graph for aeq II values. This discrepancy is believed to be related to the measurement method used in the test to obtain the  $\delta$ II strain. Being used

in the work a dial gauge positioned in the middle of the specimen, which was very difficult to follow because it is translated from small deformations. Some authors, such as De Moura et al.(2010), used LVDT's mechanical sensors in their work, which allowed them to find more coherent values for the equivalent crack length in mode II (aeq II).

## 5. REFERENCES

- American Society for Testing and Materials International, ASTM D6671/D6671M, 2015: *Standard Test Method for Mixed Mode I-Mode II Interlaminar Fracture Toughness of Unidirectional Fiber Reinforced Polymer Matrix Composites*, West Conshohocken, United States of America.
- Crews, J. H. and Reeder, J. R., 1998. "A Mixed - Mode Bending Apparatus for Delaminations Testing". Nasa Technical Memorandum 100662.
- De Moura, M.F.S.F., Oliveira, J.M.Q., Morais J.J.L., and Xavier, J., 2010. "Mixed-mode I/II wood fracture characterization using the mixed-mode bending test". *Engineering Fracture Mechanics*. v. 77, pp. 144–152.
- De Moura, M.F.S.F., Gonçalves, J.P.M., Chousal, J.A.G., and Campilho, R.D.S.G., 2008. "Cohesive and Continuum Mixed-Mode Damage Models Applied to the Simulation of the Mechanical Behaviour of Bonded Joints." *International Journal of Adhesion and Adhesives*. v.28, n.8, pp. 419-426
- Esteves, V.H.C. 2019. "*Determinação da Tenacidade de um Adesivo em Solicitações de Modo Misto (I+II)*". M.Sc. dissertation, Faculdade de Engenharia da Universidade do Porto, Porto, Portugal.
- Neto, R. M. C., 2017. "*Análise numérica e experimental de juntas coladas em duas configurações: junta de cisalhamento simples e junta de carregamento combinado*". M.Sc. dissertation, Instituto Politécnico, Universidade do Estado Rio de Janeiro, Nova Friburgo, Brazil.
- Nunes, F. A. A., 2017. "*Estudo numérico da fratura em modo misto de juntas adesivas pelo ensaio Asymmetric Tapered Double-Cantilever Beam*". M. Sc. Dissertation, Instituto Superior de Engenharia do Porto, Porto, Portugal.
- Sampaio, E.M., 1998. "*Um modelo de dano em juntas coladas*". Ph. D. thesis, Universidade Federal do Rio de Janeiro, Rio de Janeiro, Brazil.

## 6. RESPONSIBILITY NOTICE

The author(s) is (are) the only responsible for the printed material included in this paper.